ISSN 0005–1144
ATKAAF 46(3–4), 123–128 (2005)

Marin Despalatović, Martin Jadrić, Božo Terzić

Identification of Induction Motor Parameters from Free Acceleration and Deceleration Tests

UDK 621.313.333
IFAC 5.5.4

Original scientific paper

In this paper, a new step-by-step approach to identify the parameters of an induction machine combining free acceleration and deceleration transient data is presented. The measurement of the stator line voltages and currents is required only. The free acceleration torque characteristic is used in order to identify the inertia and to avoid the influence of the harmonic fields effect on the identification accuracy. The rotor resistance is identified from both free acceleration and deceleration transients data, and in that way the skin effect factor is determined. The identification results are compared with the motor parameters obtained by performing locked-rotor and no-load tests.

Key words: induction motor, measurement, modeling and simulation, parameter identification

1 INTRODUCTION

Induction machine models used for steady-state and transient analyses require machine parameters that are usually considered design parameters or data. For most small machines with cast-aluminium rotors the only available data appear on their nameplates, and the validity of the manufacturer data for these machines might be questionable, particularly for the rotor resistance because the manufacturing process affects the rotor bars conductivity. The exact knowledge of all machine parameters is very important for indirect field oriented control. A mismatched set of parameters will degrade the response of torque control [1]. Another application area for the more precise knowledge of the machine parameters is the calculation of optimal operating point for some important applications, such as traction drives [2]. On-line identification usually takes a lot of computation time. Therefore it is desirable to determine most of the parameters off-line, so that on-line identification can confine to the equivalent rotor resistance, which varies during operation due to unknown change in rotor temperature, becoming a lot faster and easier.

Traditionally, the induction machine parameters were obtained by performing locked-rotor and no-load tests. The main disadvantage of this method is that the motor has to be locked mechanically and the temperatures of the stator winding and rotor cage have to be measured. Recently, system identification techniques have been introduced to estimate the model parameters of an induction machine using standstill frequency-domain or time-domain response data, [3–8]. In [3], where the standstill frequency-domain method is used, measured magnitude and phase angle response between 0.01 and 500 Hz are used to estimate the parameter values. In time-domain parameter estimation methods, the measured transient responses of the stator voltages and currents are utilized for model parameter estimation, and the tests have been done by applying a different kind of voltage sources (dc, ac or an ac signal which is magnitude modulated, [4–7]). In [5] an attempt was made for identification of induction machine parameters from startup transient data, but the methods presented in that paper were restricted to wound rotor or very small squirrel-cage motors. Namely, when the startup test is performed on the squirrel-cage motor at the rated frequency, the skin effect can heavily influence on the accuracy of the rotor resistance. Additionally, the effect of harmonic fields can influence on the accuracy of the rotor resistance and inertia, particularly when the small squirrel-cage motors are tested, as it was discussed in [6].

2 IDENTIFICATION PROCEDURE BASED ON FREE ACCELERATION TEST

The dynamic model of a wound rotor induction machine in the stator reference frame, assuming the stator and rotor transient reactance equal, [6], may be expressed

$$\begin{aligned}\bar{u}_s &= \frac{R_s}{L_s'}\bar{\psi}_s - \frac{R_s}{L_s'}\sqrt{1-\frac{L_s'}{L_s}}\,\bar{\psi}_r + \frac{\mathrm{d}\bar{\psi}_s}{\mathrm{d}t}\\ 0 &= \left[\frac{R_r}{L_s'} - jp\omega\right]\bar{\psi}_r - \frac{R_r}{L_s'}\sqrt{1-\frac{L_s'}{L_s}}\,\bar{\psi}_s + \frac{\mathrm{d}\bar{\psi}_r}{\mathrm{d}t}\\ J\frac{\mathrm{d}\omega}{\mathrm{d}t} &= \frac{3p}{2}\frac{\sqrt{1-L_s'/L_s}}{L_s'}\left|\bar{\psi}_r\times\bar{\psi}_s\right|.\end{aligned} \qquad (1)$$

The necessary parameters to specify model (1) are: the stator resistance, R_s, the stator inductance, L_s, the transient inductance, L_s', the rotor resistance, R_r, and the inertia, J. All these parameters can be determined from the free acceleration test data using the least squares estimation algorithm [5]. But when the squirrel-cage induction motor is under the test, the skin effect and the harmonic fields effect can influence on the accuracy of the rotor resistance and inertia [6, 9]. This shortcoming can be overcome if a step-by-step approach is used, instead of the procedure proposed in [5] where all parameters are identified in one step using complete data set. The step-by-step approach proposed in [6] gives the identification results for R_s, R_r and J which are slightly depended on the wideness of incomplete data set used for estimation procedure. This influence is due to both the skin effect and harmonic fields effect. The identification procedure proposed in [6] can be improved if R_s is determined separately by the dc test, what is common for the induction motor identification procedures [2, 4, 8].

During the motor free acceleration test the stator voltages and currents are measured using Hall-effect sensors (Figure 1). Due to inevitable measurement noise the measured *abc* stator voltages and currents are filtered with a low pass filter and after that transformed into the $\alpha\beta$ variables of the stator reference frame.

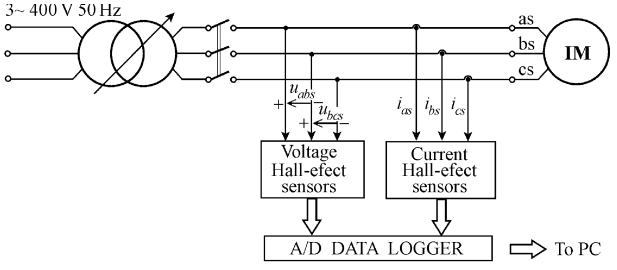

Fig. 1 Laboratory model for startup transient measurement

2.1 Determination of inertia

When the stator resistance is known, and since its change during motor free acceleration is negligible, the inertia can be obtained from the test measurements by numerically solving the following equations [10, 11]

$$\begin{aligned}\psi_\alpha &= \int_0^t (u_\alpha - R_s i_\alpha)\mathrm{d}t\\ \psi_\beta &= \int_0^t (u_\beta - R_s i_\beta)\mathrm{d}t\end{aligned} \qquad (2)$$

$$T_e = \frac{3}{2}p(\psi_\alpha i_\beta - \psi_\beta i_\alpha) \qquad (3)$$

$$J = \frac{p}{\omega_s}\int_0^{t_a} T_e\mathrm{d}t \qquad (4)$$

where p is the number of pole pairs and ω_s is stator angular frequency.

The integration boundary t_a in (4) is determined from the condition $\omega = \omega_s/p$ and it can be obtained from the free acceleration torque characteristic (Figure 2). The torque characteristic shown in Figure 2 includes influence of the both skin effect and harmonic fields effect, so from measured data by applying (2)–(4) the inertia is correctly obtained. For the purpose of verification of the described procedure the startup tests were performed for supply voltages in range 140–420 V. The results dispersion for the inertia was within ±1.5 % of the mean value.

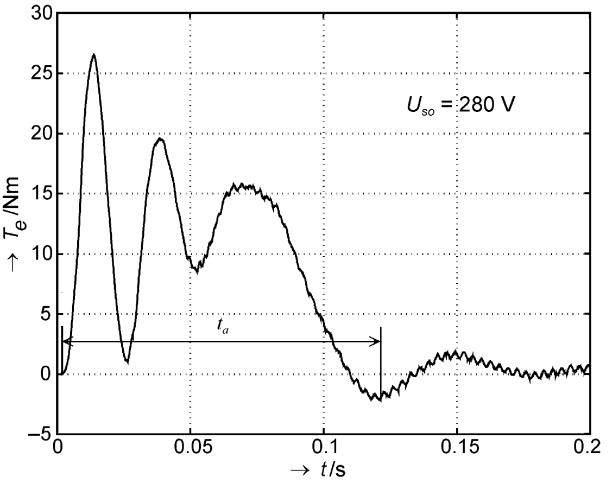

Fig. 2 The free acceleration torque characteristic

2.2 Estimation of rotor resistance and transient reactance

Neglecting R_s, reactance X_s can be determined using the end part of data set, $X_s = U_s/I_s$, where U_s, I_s are rms stator voltage and current value, respectively.

Now, when R_s, X_s and J are known, R_r and L_s' can be estimated from (1). For that purpose Levenberg-Marquardt least squares estimation algorithm is applied on the α- and β-components of the stator currents. Generally, optimization problems can take

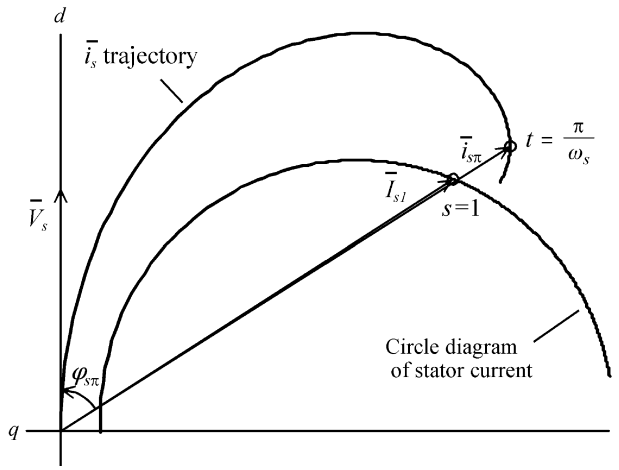

Fig. 3 Comparison of transient current space vector in $t=\pi/\omega_s$ and stationary current space vector at locked-rotor condition

many iterations to converge and can be sensitive to numerical problems such as truncation and round-off error in the calculation of finite-difference gradients. The use of less stringent termination criteria in the early stages of an optimization problem can also reduce computation time. Most optimization problems benefit from good initial guesses. This improves the execution efficiency and can help locate the global minimum instead of a local one.

Guesses for R_r and X_s' can be evaluated from the stator current space vector, obtained from data set at $\omega_s t=\pi$ (Figure 3). At the very beginning of free acceleration vector $\bar{i}_s$ may be approximated by analytic solution, which are obtained assuming locked-rotor condition. In the synchronously rotating reference frame, if the vector $\bar{u}_s$ is lying in the d-axis and the magnetizing current is neglected, vector $\bar{i}_s$ (at locked-rotor condition) may be approximated by [12]

$$\bar{i}_s = \bar{I}_{s1}(1-e^{-j\omega_s t}e^{-t/T}) \tag{5}$$

where $\bar{I}_{s1}$ is the stationary current space vector at locked-rotor condition, and T is the locked-rotor time constant. This time constant may be expressed

$$T = \frac{X_s'}{(R_s+R_r)\omega_s} = \frac{\tan\varphi_{s1}}{\omega_s} \tag{6}$$

where φ_{s1} is the angle between voltage and current at stationary locked-rotor condition. From (5), after substituting $\omega_s t=\pi$, we obtained

$$\bar{I}_{s1} \approx \frac{\bar{i}_{s\pi}}{1+e^{-\pi/\omega_s T}} \tag{7}$$

where subscript π denotes transient current space vector in $t=\pi/$ s. The trajectory of $\bar{i}_s$ and stationary current space vector $\bar{I}_{s1}$ obtained by measurements confirmed that the transient current space vector in $t=\pi/\omega_s$ ($\bar{i}_{s\pi}$) are practically collinear with $\bar{I}_{s1}$. Thus, from $\varphi_{s\pi}=\varphi_{s1}$

$$T \approx \frac{\tan\varphi_{s\pi}}{\omega_s} \tag{8}$$

where $\varphi_{s\pi}$ (the angle between $\bar{i}_{s\pi}$ and $\bar{u}_s$) is obtained from data set. It is important to note that $\varphi_{s\pi}$ does not depend on the reference frame being used. So, the guesses for R_r and X_s' are given by

$$\begin{aligned} R_r &= \frac{\sqrt{2}U_s}{|\bar{I}_{s1}|}\cos\varphi_{s\pi} - R_s \\ X_s' &= \frac{\sqrt{2}U_s}{|\bar{I}_{s1}|}\sin\varphi_{s\pi} \end{aligned} \tag{9}$$

where $\varphi_{s\pi}$ and $\bar{I}_{s1}$ are determined from measured data set transform in stator reference frame.

Since R_r changes as rotor speed is increasing, it is necessary to use the shortest possible data set length at the beginning of motor acceleration. This way the best estimate for R_r is obtained which correspond to the steady state locked-rotor condition.

To perform free acceleration test, the induction motor, 2.2 kW, 1400 min^{-1}, 400 V, 5 A, 50 Hz, is started at no-load by applying three-phase ac power and identification results for R_r and L_s' are compared with those obtained by performing locked-rotor and no-load tests (Table 1). A very good match for L_s' is obtained. Estimated R_r is approximately 6 % lower than the value obtained by locked-rotor test. This is probably due to eddy-currents in the rotor bars which are not taken into consideration in the machine model. A comparison of the current produced by the simulation with the estimated parameters is shown in Figure 4. One can see a mismatch between measurement and simulation caused by the model inaccuracy. In [6] it is proved that much better match between measured and simulated current can be obtained but with less accurate parameters.

Table 1 **Comparison of motor parameters for identification method and standard test procedure**

Parameter	$U_s=155$ V, $f_s=50$ Hz, $\vartheta=27$ °C	
	Step-by-step Identification Procedure	No-Load and Locked-Rotor Tests
R_s, Ω	–	3.01*
R_r, Ω	3.02	3.2
X_s', Ω	8.43	8.67
X_s, Ω	119	122
J, kgm^2	0.0078	0.0080**

*DC Test, **Manufacturer value

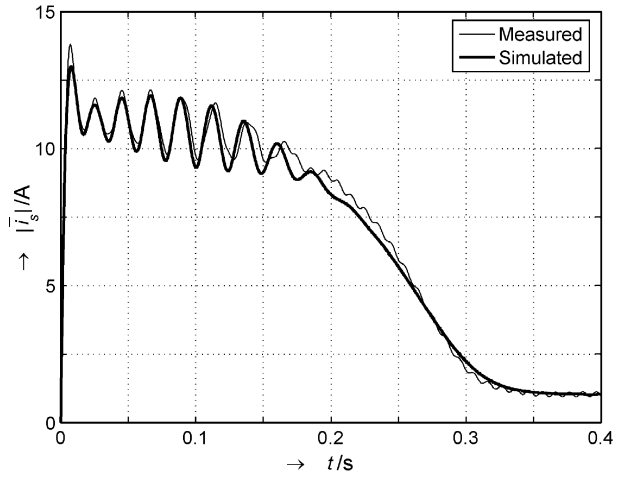

Fig. 4 Comparison of measured and simulated stator current

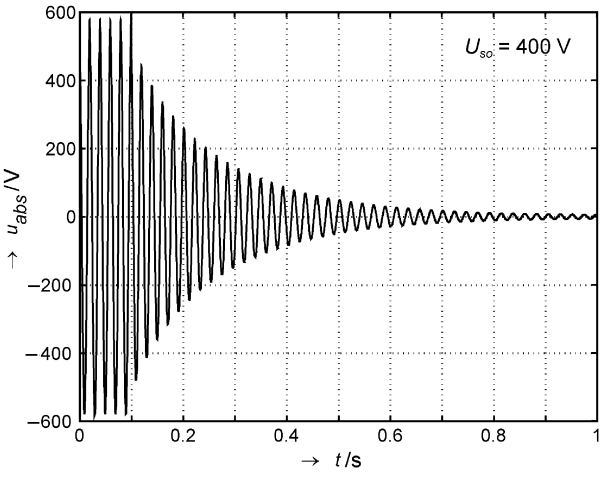

Fig. 5 Raw signal of stator line-to-line voltage

In order to avoid the influence of the temperature change on the rotor resistance, the locked--rotor test of a very short duration was performed (a little bit longer than the settling time). The stator currents and voltages were recorded and used to calculate the energy given to the rotor

$$W_{\text{rotor}} = \frac{3}{2}\int_0^{T_t}\left[\,(u_\alpha i_\alpha + u_\beta i_\beta)\; - R_s(i_\alpha^2 + i_\beta^2)\,\right]\mathrm{d}t. \quad (10)$$

Assuming that complete energy is accumulated in the rotor cage, the raise of the rotor cage temperature was calculated. In that way it was proved that the change of the rotor resistance, during performed locked-rotor tests, was negligible.

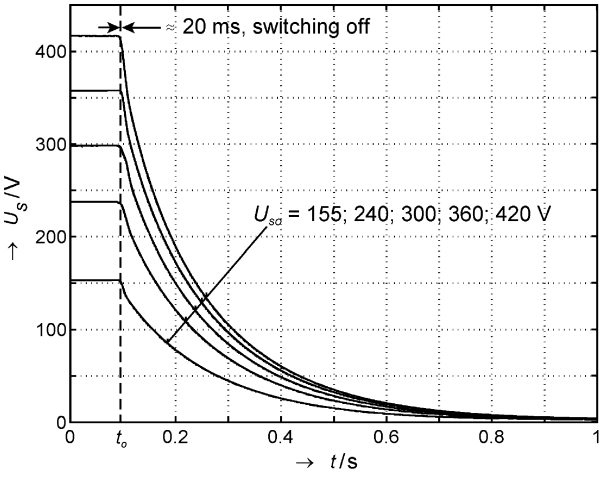

Fig. 6 Stator voltages during deceleration tests for different supply voltages

3 ROTOR TIME CONSTANT IDENTIFICATION

In order to obtain the rotor time constant, and rotor resistance without skin effect influence, free deceleration test is performed. The experimental arrangement of the test is the same as that shown in Figure 1, but the stator voltages are recorded only. The raw signal and rms values (performed with different supply voltages) of the stator line-to-line voltages are shown in Figure 5 and Figure 6, respectively.

At all tests, the motor was switched off from power supply in $t_o = 0.1$ s. After switching off the stator voltage is decaying according to the rotor open circuit time constant, T_r, and is also dependent on the rotor speed. During deceleration test the stator voltage space vector in the stator reference frame may be expressed [12]

$$\bar{u}_s = \frac{\mathrm{d}\bar{\psi}_s}{\mathrm{d}t} = \frac{L_m}{L_r}\bar{\psi}_{r0}\left(jp\omega - \frac{1}{T_r}\right)e^{-\frac{t}{T_r}}\,e^{j\vartheta} \quad (11)$$

where ϑ is the angle between the stator and rotor reference frame. For the purpose of this analysis the second term in parentheses in (11) may be neglected. Thus, the rms stator voltage may be written as

$$U_s = C\,\omega\, e^{-\frac{t}{T_r}} \quad (12)$$

where C is unknown constant. To calculate T_r from (12), $\omega(t)$ should be known. The rotor speed time characteristic, $\omega(t)$, can be calculated from the angle ϑ

$$\omega = \frac{1}{p}\frac{\mathrm{d}\vartheta}{\mathrm{d}t} \approx \frac{1}{p}\frac{\Delta\vartheta}{\Delta t} = \frac{1}{p}\frac{\vartheta(t_{i+1}) - \vartheta(t_i)}{t_{i+1} - t_i} \quad (13)$$

where ϑ is obtained from the measured voltages

$$\vartheta = \tan^{-1}\frac{\sqrt{3}\,u_{bcs}}{u_{abs} - u_{cas}}. \quad (14)$$

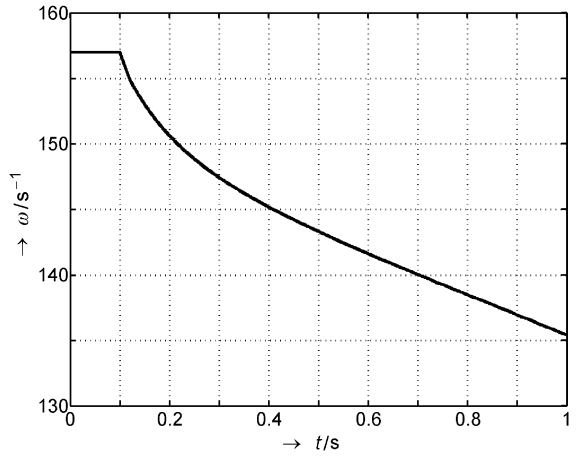

Fig. 7 Rotor angular speed which correspond to Figure 5

In order to obtain a high quality estimate of the rotor speed (Figure 7), before differentiating the angle ϑ in (13), it is necessary to unwrap phase in (14) and after that apply a digital low pass filter to eliminate the influence of the voltage harmonics.

Since in (12) two unknowns (T_r, C) exists, it is necessary to chose two points on $U_s(t)$ characteristic. That way system of two exponential equations can be setup. The following solution for T_r is obtained

$$T_r = \frac{\Delta t}{\ln\dfrac{U_{s1}}{U_{s2}} - \ln\dfrac{\omega_1}{\omega_2}}. \qquad (15)$$

It is important to note that a very short part of the data set (approximately during first period after switching off) should be excluded from analysis due to switching off effects.

During deceleration test T_r is changeable due to saturation. Because of that time interval $\Delta t = t_2 - t_1$ in (15) should be short enough so that T_r may be assumed to be constant. For that reason a sliding window of length equal to one electrical period was defined and the result was pined to the middle point of the window. By applying sliding window technique, time dependence of rotor time constant, $T_r(t)$, was obtained. By combining the characteristics $T_r(t)$ and $U_s(t)$, and eliminating the time, the rotor time constant dependence on stator voltage, $T_r(U_s)$, shown in Figure 8 was obtained. Described procedure has been applied on the data sets obtained for different supply voltages. A very good overlapping (which cannot be seen in Figure 8) of the $T_r(U_s)$ characteristics has been achieved.

Figure 8 shows influence of saturation on rotor time constant. Namely, if rotor resistance is assumed to be constant, the rotor time constant, $T_r = L_r/R_r$, directly depends on L_r which changes with U_s due to saturation.

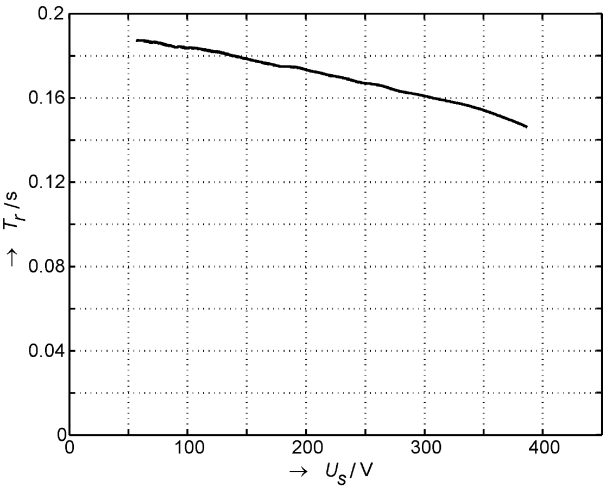

Fig. 8 Rotor time constant dependence on stator voltage

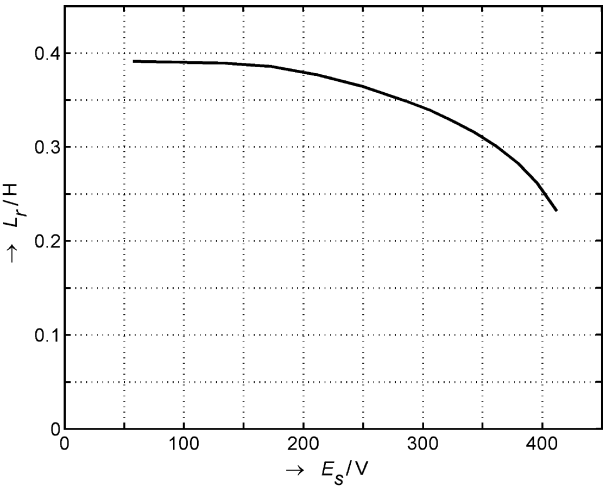

Fig. 9 Rotor inductance obtained from no-load test

By combining Figure 8 with Figure 9, which shows rotor inductance obtained from no-load test assuming $L_r = L_s$, rotor resistance can be calculated

$$R_r = \frac{L_r(E_s)}{T_r(U_s)} \qquad (16)$$

where $U_s = E_s$.

By applying (16) for different voltages the mean value of the rotor resistance equal to 2.16 Ω is obtained and the results dispersion is within ±5 %. Thus, this way calculated rotor resistance is approximately 30 % lower than the value determined by performing the locked-rotor test (Table 1). Also the rotor resistance obtained from (16) is approximately 15 % lower than the design (manufacturer) value what is probably due to uncertainty in the cast-aluminium rotor specific conductivity.

4 CONCLUSION

Free acceleration and deceleration tests seem to be very suitable for parameter identification of the small induction machines. But the motor model inaccuracy can cause a considerable estimation error, particularly in the inertia and rotor resistance. In order to avoid this inaccuracy, a new simple and effective algorithm for determination of the inertia has been proposed. This algorithm, which is based on previous knowledge of the stator resistance and the free acceleration test, yields very accurate results for the inertia.

Estimated results for the rotor resistance and transient reactance have been compared with those obtained from locked-rotor and no-load test. A very good match for the transient reactance is obtained. Some discrepancy in the rotor resistance results can be explained by the influence of the eddy-currents in the rotor bars which are not taken into consideration in the machine model.

A new technique based on deceleration test for determination of the rotor time constant has been proposed and investigated. Based on the results of the both free acceleration and deceleration tests the dc current rotor resistance is obtained. This value of the rotor resistance is approximately fifteen percent lower than the design one. This is due to uncertainty in the cast-aluminium rotor specific conductivity. Thus, described procedure can be used for a verification of the cast-aluminium rotor specific conductivity.

REFERENCES

[1] J. Holtz, T. Thimm, **Identification of the Machine Parameters in a Vector-Controlled Induction Motor Drive.** IEEE Trans. Ind. Applicat., Vol. 27, No. 6, pp. 1111–1118, Nov./Dec. 1991.

[2] N. R. Klaes, **Parameter Identification of an Induction Machine with Regard to Dependencies on Saturation.** IEEE Trans. Ind. Applicat., Vol. 29, No. 6, pp. 1135–1140, Nov./Dec. 1993.

[3] J. R. Willis, G. J. Brock, J. S. Edmonds, **Derivation of Induction Motor Models from Standstill Frequency Responses Test,** IEEE Trans. Energy Conversion, Vol. 4, pp. 608–615, Dec. 1989.

[4] S.-I. Moon, G. Keyhani, **Estimation of Induction Machine Parameters from Standstill Time-Domain Data,** IEEE Trans. Ind. Applicat., Vol. 30, No. 6, pp. 1111–1118, Nov./Dec. 1994.

[5] S. R. Shaw, S. B. Leeb Edmonds, **Identification of Induction Motor Parameters from Transient Stator Current Measurements,** IEEE Trans. Ind. Electronics, Vol. 46, No. 1, pp. 139–149, Feb. 1999.

[6] M. Jadrić, M. Despalatović, B. Terzić, **Identification of Induction Motor Parameters from Free Acceleration Test Measurements,** EPE-PEMC, Cavtat, Croatia, September 9–11, 2002.

[7] H. Razik, C. Defranoux, A. Rezzoug, **Identification of Induction Motor using a Genetic Algorithm and a Quasi-Newton Algorithm,** CIEP, pp. 65–70, Acapulco, Mexico, October 15–19, 2000.

[8] J.-K. Seok, S.-I. Moon, A.-K. Sul, **Induction Machine Parameter Identification using PWM Inverter at Standstill.** IEEE Trans. Energy Conversion, Vol. 12, No. 2, pp. 127–132, June 1997.

[9] F. Taegen, **Die Bedeutung der Läufernutschlitze für die Theorie der Asynchronmaschinen mit Käfigläufer.** Archiv für Elektrotechnik, Bd. 48, H. 6, S. 373–385, 1964.

[10] J. Hu, B. Wu, **New Integration Algorithms for Estimating Motor Flux over a Wide Speed Range.** IEEE Trans. Power Electronics, Vol. 13, pp. 969–977, Sept. 1998.

[11] W. H. Press, S. A. Teukolsky, W. T. Vetterling, B. P. Flannery, **Numerical Recipes in Fortran: The Art of Scientific Computing.** Cambridge University Press, 1992.

[12] M. Jadrić, B. Frančić, **Dynamics of Electrical Machines** (in Croatian), Graphis, Zagreb, 1997.

Identifikacija parametara asinkronog motora na temelju pokusa zaleta i zaustavljanja. U ovom je radu predstavljen jedan novi postupak za identifikaciju parametara asinkronog motora koji se temelji na pokusima zaleta i zaustavljanja neopterećenog motora. Pritom se zahtjeva samo mjerenje statorskih napona i struja. Momentna karakteristika motora dobivena iz mjerenja u pokusu zaleta koristi se za određivanje inercije. Na taj način izbjegnut je utjecaj viših prostornih harmonika polja na točnost identifikacijskog postupka. Otpor rotora određuje se iz pokusa zaleta i iz pokusa zaustavljanja, čime je posredno određen i faktor potiskivanja struje. Rezultati dobiveni identifikacijskim postupkom uspoređeni su s parametrima motora dobivenima iz pokusa praznog hoda i kratkog spoja.

Ključne riječi: asinkroni motor, identifikacija parametara, mjerenje, modeliranje i simulacija

AUTHORS' ADDRESSES

Marin Despalatović, dipl. ing.
Dr. sc. Martin Jadrić, red. prof.
Dr. sc. Božo Terzić, izv. prof.

Fakultet elektrotehnike strojarstva i brodogradnje
Sveučilišta u Splitu, Zavod za elektroenergetiku
Ruđera Boškovića bb, 21000 Split, Hrvatska

E-mail: despi@fesb.hr
mjadric@fesb.hr
bterzic@fesb.hr

Received: 2005-12-19